The kinematics of directional control in the fast start of zebrafish larvae

Arjun Nair, Grigor Azatian and Matthew J. McHenry*

ABSTRACT

Larval fish use the 'fast start' escape response to rapidly evade the strike of a predator with a three-dimensional (3D) maneuver. Although this behavior is essential for the survival of fishes, it is not clear how its motion is controlled by the motor system of a larval fish. As a basis for understanding this control, we measured the high-speed kinematics of the body of zebrafish (*Danio rerio*) larvae when executing the fast start in a variety of directions. We found that the angular excursion in the lateral direction is correlated with the yaw angle in the initial stage of bending (stage 1). In this way, larvae moved in a manner similar to that reported for adult fish. However, larvae also have the ability to control the elevation of a fast start. We found that escapes directed downwards or upwards were achieved by pitching the body throughout the stages of the fast start. Changes in the pitching angle in each stage were significantly correlated with the elevation angle of the trajectory. Therefore, as a larva performs rapid oscillations in yaw that contribute to undulatory motion, the elevation of an escape is generated by more gradual and sustained changes in pitch. These observations are consistent with a model of motor control where elevation is directed through the differential activation of the epaxial and hypaxial musculature. This 3D motion could serve to enhance evasiveness by varying elevation without slowing the escape from a predator.

INTRODUCTION

Fish evade predators by executing a 'fast start' escape response that is rapid, yet permits swimming in a controlled direction (Domenici and Blake, 1997). This behavior enables a fish to survive an encounter with a predator (Walker et al., 2005). However, it remains unclear what mechanics and neurophysiology facilitate this directional control. Zebrafish larvae (*Danio rerio*) present unique opportunities to test hypotheses on this subject, but the morphology of larvae is distinct from adults and they are at least an order of magnitude smaller. Therefore, larval fish have the potential to deviate from the adult models of neuromechanical control (e.g. Foreman and Eaton, 1993). One feature that has not been reported for adult fish is the ability of larvae to control the elevation of a fast start. Elevation is the angular deviation from the horizontal plane in an earth-bound frame of reference and its control allows larvae to dive away from a predator (Stewart et al., 2014). In the interest of understanding how motor systems facilitate this control, the present

Department of Ecology & Evolutionary Biology, University of California, Irvine, CA 92617, USA.

*Author for correspondence (mmchenry@uci.edu)

study measured the three-dimensional (3D) kinematics of larval zebrafish when executing fast starts that vary in elevation.

The fast start is a classic behavior for studying motor control in vertebrates. Escape responses like the fast start were thought to operate as a 'fixed-action pattern' with stereotyped kinematics that are initiated by a threshold stimulus (Barlow, 1968). Consistent with this idea, the fast start follows a characteristic sequence that has been described in three stages. In stage 1, the fish unilaterally contracts its muscles, which bends the body into a 'C' shape and causes the head to yaw. In stage 2, the head rotates in the opposite direction through the action of contralateral muscles, as the body straightens and accelerates forward. This is followed by the rapid undulatory swimming of stage 3 (Weihs, 1973). Variation in the speed and degree of body rotation within each of these stages generates escape kinematics with a variable azimuth, which is the angular heading on the horizontal plane. The azimuth has been shown to depend on the intensity and direction of a stimulus (e.g. Eaton et al., 1981; Peterson, 1984; Eaton et al., 1988; Nissanov et al., 1990; Eaton et al., 1991; Liu and Fetcho, 1999). Therefore, the fast start exhibits a degree of control that is beyond the stereotyped motion of a fixed-action pattern.

Ideas about the directional control of the fast start are largely based on research on adult goldfish (*Carassius auratus auratus*). These studies have demonstrated that the fish rotates away from a threat anterior to the body by first creating a large stage 1 yaw. This is followed by less rotation in the opposite direction during the acceleration of stage 2. In contrast, a caudal stimulus generates a relatively modest yaw over both stages to direct swimming forward (Eaton et al., 1988; Eaton and Emberley, 1991). As a consequence of these patterns, the azimuth of an escape is correlated with the yaw angles generated in stages 1 and 2. This is an observation that is consistent with the hypothesis that the reticulospinal neurons that control a fast start are activated in a manner that depends on the relative position of a stimulus (Foreman and Eaton, 1993).

Zebrafish larvae offer opportunities to test these ideas with visualization techniques that have benefited from the transparent bodies of these animals. For example, calcium imaging revealed that three reticulospinal neurons are activated by a rostral stimulus, whereas only one neuron is activated by a caudal stimulus (O'Malley et al., 1996). These results support the control model that was based on adult goldfish (Foreman and Eaton, 1993). Further opportunities in this area are developing with a growing toolkit of transgenic lines for zebrafish that permit functional imaging and optogenetics (e.g. Fetcho et al., 2008; Nakayama and Oda, 2004; Akerboom et al., 2012). Despite these advances, fundamental aspects of the behavior remain unresolved for larval fish and it is not clear how the body moves to direct the fast start in three dimensions (Müller and van Leeuwen, 2004; Stewart et al., 2014). It is for these reasons that the present study aimed to measure the 3D body kinematics of zebrafish larvae for fast starts that vary in direction.
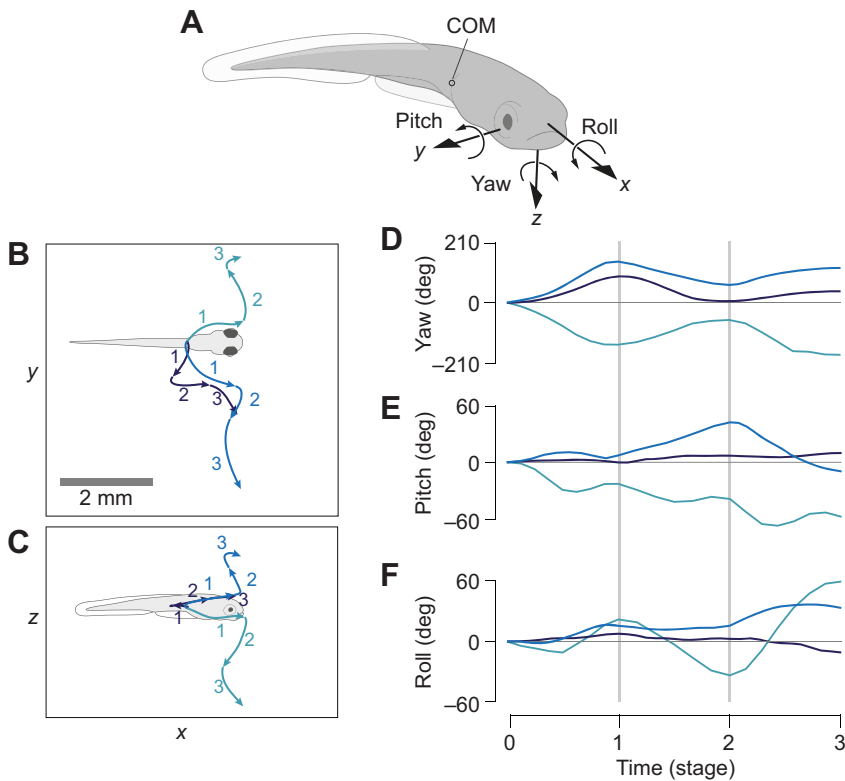
Fig. 1. Three-dimensional trajectories of the fast start in zebrafish larva. (A) A schematic diagram of the coordinate system used for the body of a larva with its Euler angles. The body's center of mass (COM) was approximated at the posterior margin of the swim bladder (Stewart and McHenry, 2010). (B,C) Trajectories of the COM during the fast start in three different directions on a horizontal (x–y) plane (B) and a vertical (x–z) plane (C). The Euler angles of the sequences shown in B and C are shown in terms of yaw (D), pitch (E) and roll (F).

MATERIALS AND METHODS

We used kinematic measurements to describe the body motion of larval zebrafish. In particular, the rotation of the head and bending of the tail were measured from high-speed recordings of fast starts that were stimulated with a jet of water. We examined how these measurements correlated with the direction of the escape trajectory in azimuth and elevation. These findings offer an observational basis for understanding how larval fish control fast start direction in three dimensions.

Animal husbandry

All experiments were performed on zebrafish larvae (*Danio rerio*, Hamilton 1922) between the ages of 5 and 7 days post-fertilization. All larvae were bred from wild-type (AB line) colonies housed in a flow-through tank system (Aquatic Habitats, Apopka, FL, USA) that was maintained at 28.5°C on a 14 h:10 h light:dark cycle. The fertilized eggs from randomized mating were cultured according to standard techniques (Westerfield, 1993).

Experiments

We recorded the 3D kinematics of escape responses with two high-speed video cameras. Larvae were recorded in an acrylic tank (a 30 mm cube) with the cameras positioned above the surface and normal to one of the walls. The cameras (FASTCAM 1024PCI, Photron, San Diego, CA, USA) recorded at 1000 frames s^{-1} and were synchronized with a transistor–transistor logic

(TTL) pulse. Larvae were visualized with transmitted illumination that was provided by two high-power LED floodlights (120 W equivalent daylight, 5000K PAR38 dimmable LED flood light bulb, Philips, Andover, MA, USA) with diffusers (100 mm×100 mm opal glass, Edmund Optics, Barrington, NJ, USA).

Zebrafish were induced to direct their escape in a variety of directions with a fluid jet. After a 15 min acclimation period, we exposed larvae to this stimulus, which was emitted from a curved capillary tube with an inner diameter of 1.1 mm. We directed this tube towards the center of the tank and positioned it either above or below the larvae. The impulsive pressure (Picospritzer II, General Valve Corporation, Fairfield, NJ, USA) was adjusted to have a 7 ms duration and a peak pressure of 14 kPa. These settings were sufficient to elicit a reaction from the larva but not displace the body.

Kinematic analysis

We performed a calibration to resolve 3D coordinates from the recordings by the two cameras. The calibration used recordings of a calibration body of a known geometry that was placed in the center of our water-filled tank. This body contained 27 distinct landmarks of known 3D position, which we designed with CAD software (SketchUp 2013, Trimble Navigation, Sunnyvale, CA, USA) and created with a 3D printer (ShapeWays, New York, NY, USA). The calibration was performed by a direct-linear transformation (Digitizing Toolkit, Hedrick, 2008) in MATLAB (version
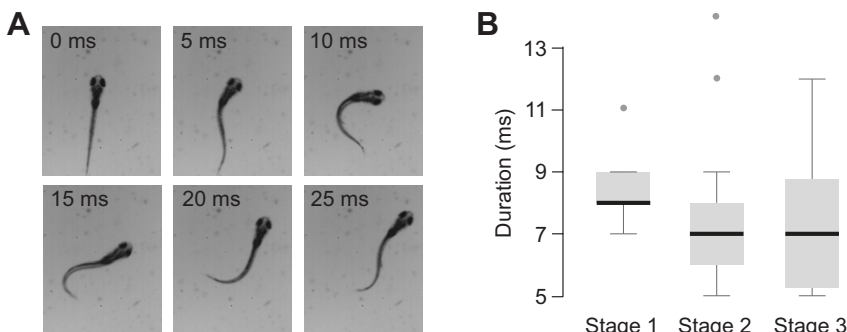
Fig. 2. The stages of a fast start. (A) Video frames of a representative fast start, recorded from a dorsal view in 5 ms intervals. A fast start is described in three stages. In stage 1, the zebrafish larva curls its body to one side, then rapidly unfurls its body in stage 2 and begins undulatory swimming away in stage 3. (B) All stages were statistically indistinguishable in duration (one-way ANOVA, P=0.70, N=15). The durations of each stage are shown with a box-and-whisker plot with the median (black line), first and third quartiles (gray box), range (whiskers) and outliers (filled circles, >2 s.d.).
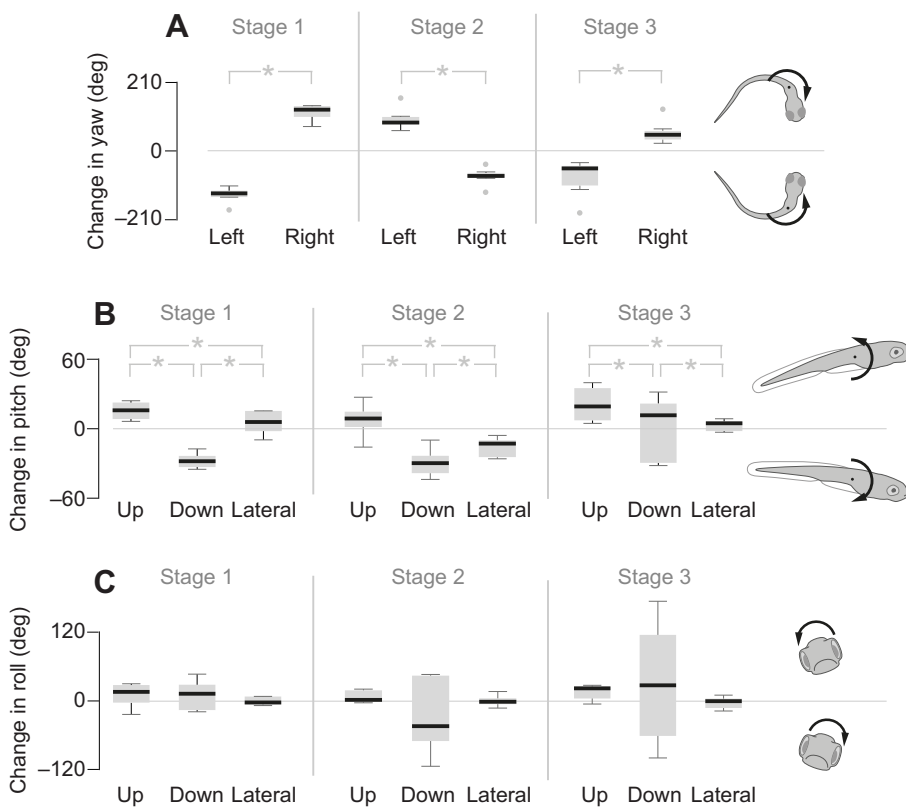
Fig. 3. Body rotation for fast starts in different directions. We measured body rotation by change in the Euler angles during each stage of the fast start. (A) Change in yaw differed significantly between fast starts that were directed to the left or right of the body for all stages ($P<0.001$, $N=15$). (B) Change in pitch differed significantly between fast starts that were directed upwards, downwards and laterally (within ±15 deg margin) from the initial orientation for all stages ($P<0.001$, $N=15$). (C) Change in roll had no significant differences between upward, downward and lateral fast starts. Each group of measurements is presented by its median (black line), first and third quartiles (gray box), range (whiskers) and outliers (filled circles, >2 s.d.), with significant differences (*) between groups.

2014a, MathWorks, Natick, MA, USA) from manually selected coordinates at landmarks on our calibration body from the two camera recordings.

Two-dimensional position data were collected from both cameras to reconstruct the 3D motion of a larva. Using custom software developed in MATLAB, the 2D coordinates from both views were collected from the body landmarks for each frame of both recordings. Software developed in MATLAB was further employed to implement all of the post-processing and statistics described below. The body landmarks consisted of the centers of both eyes and the posterior margin of the swim bladder. For the tail, we recorded a series of positions (8–20 points, depending on the curvature of the tail and the perspective of the camera) along the dorsal and ventral edges, which were visible because of lines of pigmentation. Position data were smoothed with splines that were implemented with a least-squares approximation ('spap2' in MATLAB) with user-defined knots to compensate for calibration error and inconsistencies in the acquisition of body landmarks. Splines were fitted to the time series of each dimension of the data for the eyes and swim bladder, as well as the spatial variation of the tail coordinates for each video frame.

We determined the rotation of the body from our measurements of the position of the head. This was achieved by defining a coordinate system with its origin at the mean position between the eyes. The y-axis of this system was directed to the right side of the body and was calculated as a unit vector that was directed from the origin to the right eye. The z-axis was calculated as the cross-product of y-axis vector and another running from the origin to the swim bladder. Finally, the x-axis was determined from the cross-product of the y- and z-axes. Angular changes in this coordinate system were defined as the Euler angles of roll, pitch and yaw, which indicated rotation around the x-, y- and z-axes, respectively. Euler angles were calculated from 3×3 rotation matrices defined with respect to the body orientation prior to the initiation of the fast start (Craig, 1989).

The timing of each stage in the fast start was determined by oscillations in yaw (Fig. 1D–F). Stage 1 was defined as the duration between the onset of motion and the first maximum or minimum of yaw, when the body curled into its initial 'C' shape. Stage 2 spanned from the end of stage 1 until the next minimum or maximum in yaw as the body unfurled. This was followed by stage 3, which continued up to the third maximum or minimum value in

yaw, as the larva undulated its body for half of a tail beat. Changes in the Euler angles were defined as the angular difference between these angles from one stage to another. The changes in Euler angles associated with different directions for the escape trajectory were statistically compared using a one-way ANOVA (comparing up, down and lateral directions) or a t-test (comparing left and right turns). Outliers were excluded from statistical tests and were determined by a two standard-deviation cut-off.

The direction of an escape was calculated from the trajectory of the swim bladder over stages 2 and 3. The posterior margin of the swim bladder approximates the body's center of mass (Stewart and McHenry, 2010) and therefore offered a measure of the prevailing direction of body motion. We found the trajectory direction by a 3D linear, least-squares fit of the position recordings between the start of stage 2 and end of stage 3. From this vector, we calculated the azimuth and elevation of the trajectory. Azimuth and elevation angles were respectively compared with changes in yaw and pitch using linear regression analysis.

We determined the motion of the tail from changes in its orientation. We solved for 19 points of even-spacing along the arclength from each spline-fit for the dorsal and ventral margins of the tail. The line segments between each pair of points for the dorsal and ventral margins were used to define a 3D plane that represented the orientation of a segment of the tail. We derived the angular excursion of this plane in lateral and dorsoventral orientations relative to the orientation of the same segment prior to the fast start.
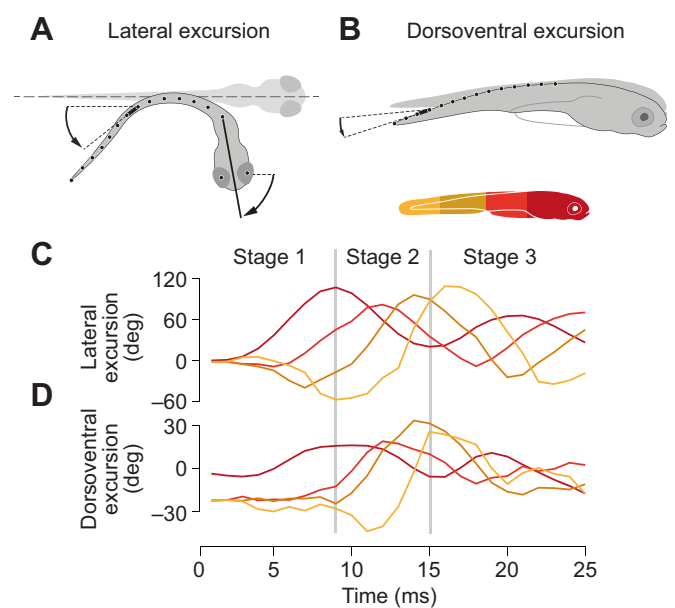
RESULTS
Body rotation

Zebrafish larvae exhibited all three stages of the fast start within view of both cameras. Using the posterior margin of the swim bladder to approximate the center of mass (Stewart and McHenry, 2010), we found that the body of a larva curled into a 'C' shape during stage 1 with little center-of-mass translation. The body then began to displace as it unfurled in stage 2, in the transition towards the undulatory swimming of stage 3 (Fig. 2A). The durations of each stage were statistically indistinguishable (one-way ANOVA: $P=0.70$, $N=15$), with each lasting about 8 ms (7.76±2.08, mean±1 s.d., $N=15$, Fig. 2B).
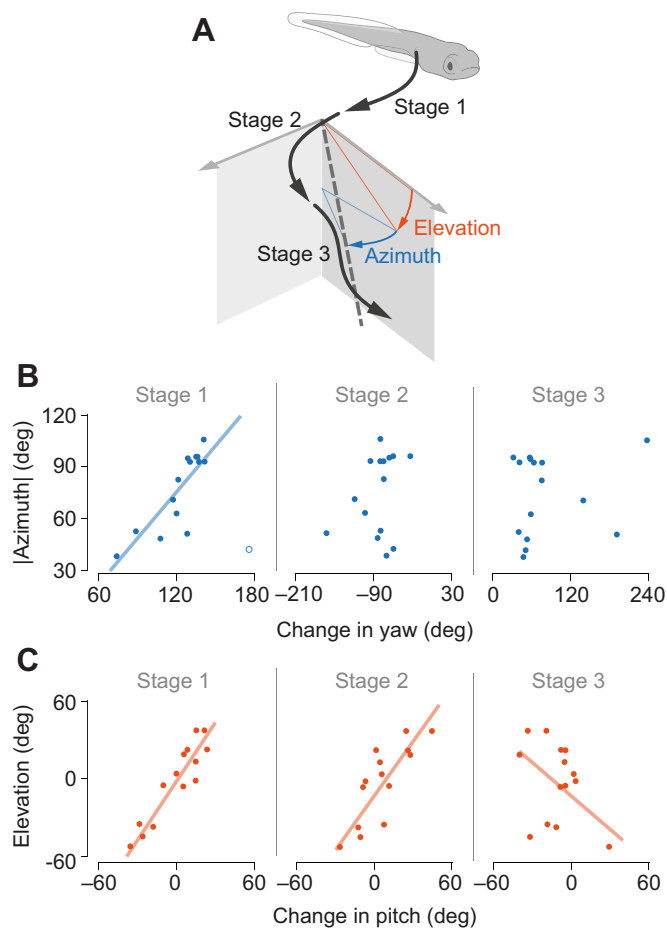
Fig. 4. The relationship between body rotation and the direction of a fast start. (A) The azimuth (in blue) and elevation (in red) of the fast start trajectory were found with a least-squares linear fit of the trajectory of stages 2 and 3. (B) Correlations between changes in yaw and the absolute value of the azimuth angle were significant for stage 1 ($P<0.001$, $r^2=0.70$, $y=0.94x-37.2$, $N=15$). (C) In contrast, changes in pitch for each stage were significantly correlated with the elevation of a fast start ($P<0.001$ for stage 1, $y=1.51x-1.85$ and stage 2, $y=1.40x-12.4$; $P=0.046$ for stage 3, $y=-0.86x-12.8$, $N=15$). In addition, the changes in pitch during stage 1 ($r^2=0.86$, $N=15$) and stage 2 ($r^2=0.68$, $N=15$) were highly predictive of variation in elevation. In contrast, change in pitch during stage 3 predicted only about one-third of variation in elevation ($r^2=0.27$, $N=15$). Outlier values are presented as open circles.

Fig. 5. Body bending during a fast start. Angular excursions of the head and tail show rotation of the body relative to the initial orientation of the body in lateral (A) and dorsoventral (B) directions. (C,D) Rotation of the head (in dark red) has been plotted over time with tail angular excursion from the anterior ($0<L<0.25$, in orange), middle ($0.25<L<0.50$, in gold) and posterior ($0.50<L<0.75$, in yellow) regions for one fast start in lateral (C) and dorsoventral (D) directions.

From the beginning of a fast start, the larvae rotated their body in the direction to which they were ultimately headed. This was indicated by our measurements of the Euler angles (yaw, pitch and roll, Fig. 1A), which were calculated from the coordinates of the eyes and swim bladder. For example, a larva moving downwards and towards the left side of the body (teal curves in Fig. 1B,C) showed changes in yaw and pitch that progressively grew more negative across all stages of the fast start (Fig. 1D,E), which was consistent with the convention of our coordinate system (Fig. 1A). The trend in pitch was apparent in stage 1, which indicates a directional bias that started at the earliest moments of an escape. This may be contrasted with an escape that remained largely on a horizontal plane (e.g. dark blue curves in Fig. 1B,C). Whilst also showing short-period and large-amplitude oscillations in yaw (Fig. 1D), the pitch angle of this response did not trend away from a zero value (Fig. 1E). Regardless of the direction of a trajectory, larvae exhibited roll that could be comparable in magnitude to pitch, but we found no

evidence that these changes were associated with the direction of the escape (Figs 1F and 3C).

Yaw and pitch varied with the escape direction. For example, fast starts to the left were characterized by a negative change in yaw for stage 1 (Fig. 3A), because the body initially curled in the ultimate direction of the trajectory (Fig. 1A). This was followed by a positive change in yaw during stage 2 and another reversal in stage 3 (Fig. 3A). In each of these stages, the differences in yaw were highly distinct (t-test: $P<0.001$, $N=15$) between escapes to the left and right. In a similar way, fast starts directed upwards, laterally and downwards were all significantly different in the changes in pitch achieved in each stage (one-way ANOVA: $P<0.001$, $N=15$, Fig. 3B). In contrast, body roll did not vary significantly between escapes of different direction (one-way ANOVA: $P>0.05$, $N=15$, Fig. 3C).

The azimuth and elevation angles of a trajectory were correlated with the rotations of the head. In particular, change in the yaw angle was correlated with the azimuth of the trajectory for stage 1 ($P<0.001$, $r^2=0.71$, $N=15$), but not in subsequent stages (Fig. 4B). The change in pitch for all stages was correlated with the elevation ($P<0.001$ for stages 1 and 2, $P=0.046$ for stage 3, $N=15$). As indicated by the coefficient of determination, most variation in elevation could be predicted from differences in the change in pitch over stages 1 ($r^2=0.87$) and 2 ($r^2=0.68$, Fig. 4C). Only about one-third of the variation in elevation could be predicted from the change in pitch over stage 3 ($r^2=0.27$). Therefore, the degree of elevation change created during a fast start is closely related to body pitching in the first two stages.

Tail kinematics
We measured tail kinematics to examine how the bending of the body related to head rotation and the direction of a fast start. From coordinates of the dorsal margin of the tail, we measured the angular
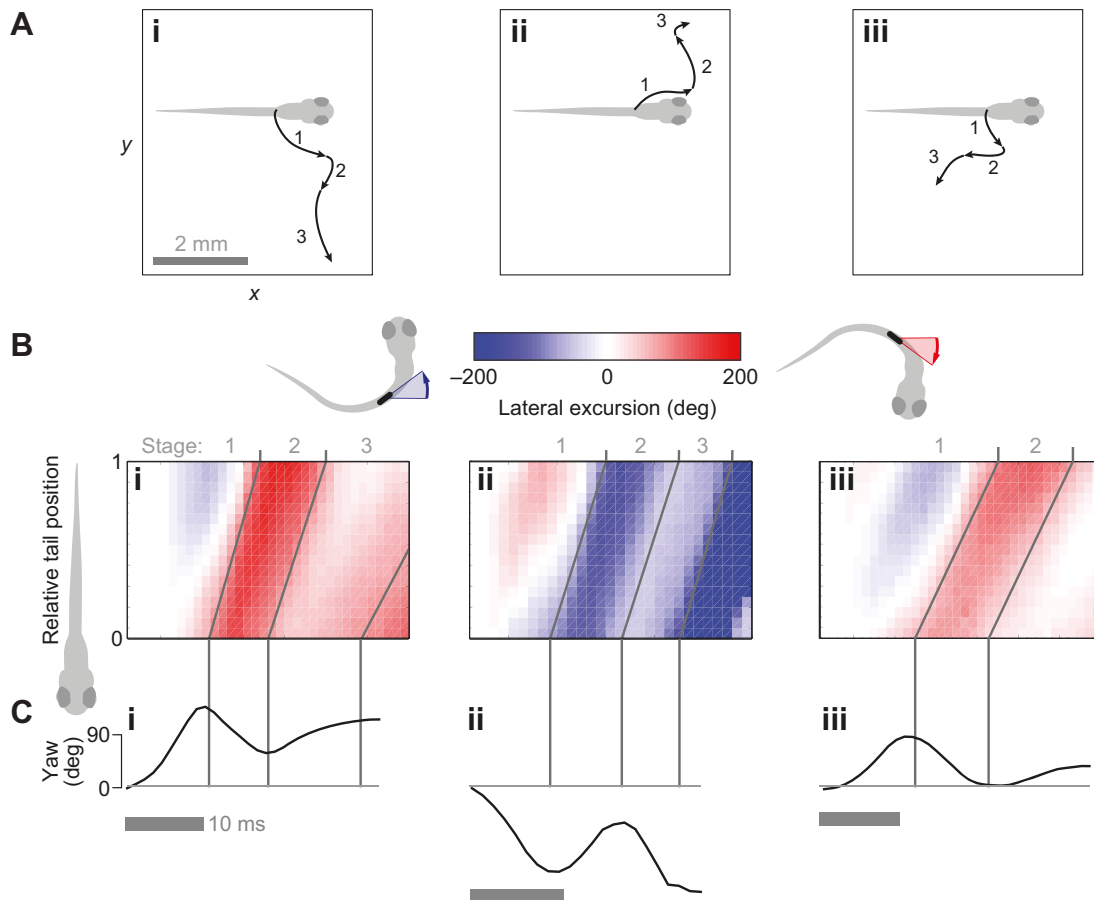
Fig. 6. Lateral bending during a fast start. The lateral tail excursion and yaw for fast start maneuvers directed towards the right (i and iii) and left (ii) of the body (the same sequences as in Fig. 1B–F). (A) The trajectories for each fast start is plotted in the horizontal plane, with arrows presenting the trajectory achieved over an individual stage. (B) From the same three fast starts depicted in A, we measured the lateral excursion of the tail, throughout its length in pseudocolor that encodes positive (in red) and negative (in blue) angles. Diagonal lines (dark gray) in each pseudocolor plot denote the transition between the stages of each fast start. (C) The corresponding measurements for the yaw of the head are shown for the same sequences as illustrated in A and B.

excursion relative to the initial orientation of the body in the lateral (Fig. 5A) and dorsoventral (Fig. 5B) directions. This provided the means to relate tail motion to the Euler angles of the head (Fig. 1A) and offered a measurement of bending with a superior signal-to-noise ratio than calculations of tail curvature. This allowed us to examine how the rapid change in the lateral excursion of the head (i.e. yaw, Fig. 1A) was reflected in the angular excursion of the tail (Fig. 5C) with a delay. A similar pattern was apparent in the dorsoventral excursion, where changes in the head (i.e. pitch, Fig. 1A) were reflected with a delay in the tail (Fig. 5D). Therefore, the tail followed a course of motion set by the head in both lateral and dorsoventral directions. Head rotation was also related to simultaneous change in the angular position of the tail in the opposite direction. This was most acute in stage 1, where positive changes in the lateral excursion of the head were mirrored by negative changes in the tail with lower magnitude (Fig. 5C).

The propagation of undulatory waves in the tail differed between escapes towards the left and right. For example, in a rightward fast start (Fig. 6Ai), the anterior region of the tail followed a positive (i.e. clockwise from a dorsal view) angular excursion (Fig. 6Bi) as the head yawed towards the right of the body (Fig. 6Ci) during stage 1. At this time, the posterior region of the tail bent in the opposite direction, with a negative (i.e. counter-clockwise) angular excursion (Fig. 6Bi). The end of stage 1 was marked by a reversal in yaw and the tail excursion created by the unfurling of the body from this

stage. Undulatory waves generated similar reversals in excursion, which marked the ending of stages 2 and 3 (Fig. 6Bi). An escape towards the left side of the body (Fig. 6Aii) showed a similar pattern, but in the opposite direction (Fig. 6Bii,Cii).

Similar differences in bending were apparent in the dorsoventral direction among responses that varied in elevation. For example, an escape upwards (Fig. 7Ai) began with a dorsal bend in the tail (Fig. 7Bi), as the head pitched in the same direction (Fig. 7Ci). The end of each stage was marked by undulatory waves in dorsoventral excursion that were initiated by the motion of the head. Similar events occurred in escapes directed downwards, but in the opposite direction (e.g. Fig. 7Aii, Bii and Cii). An escape trajectory that was restricted to planar motion (Fig. 7Aiii) occurred with relatively minor variation in pitch (Fig. 7Ciii) and dorsoventral angular excursion (Fig. 7Biii). Therefore, the dorsoventral motion of the tail largely propagated from the pitching apparent in the motion of the head at each stage in the fast start.

We examined relationships between the extent of the tail's angular motion and the direction of the fast start. We found significant correlations ($P \ll 0.001$, $N=15$) between the lateral excursion of the posterior region of the tail ($0.9L$, where L is the length of the tail) and the azimuth of the trajectory for all three stages (Fig. 8A). We similarly found significant correlations ($P<0.001$, $N=15$) between the change in dorsoventral excursion of each stage and elevation for the posterior region (Fig. 8B). The
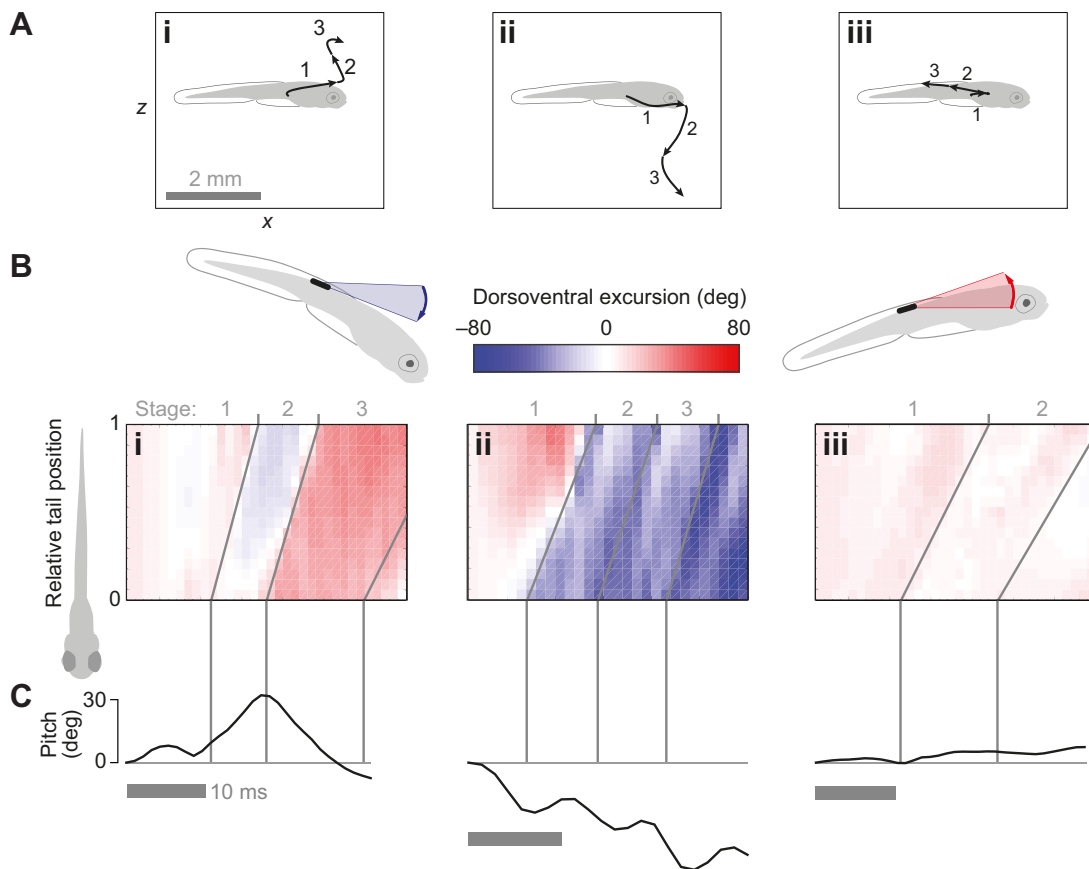
Fig. 7. Dorsoventral bending during a fast start. (A,B) The dorsoventral excursion during fast starts directed (i) upwards, (ii) downwards and (iii) laterally (the same sequences as in Fig. 1B–F and Fig. 6). (A) The trajectory for each fast start plotted in the vertical plane with arrows that differentiate each stage. (B) The dorsoventral excursion of the body changes with bending that is directed downwards (in blue) and upwards (in red). Diagonal lines (dark gray) in each pseudocolor plot denote the transitions between the stages. (C) Measurements of the corresponding pitch angle for the head are shown for the same sequences as illustrated in A and B.

anterior region was also significantly correlated with elevation for stages 1 and 2. These correlations with elevation were positive for the anterior region, where the tail rotated in the same direction as the head and ultimate heading of the trajectory. The negative correlations for the posterior region were the result of the tail rotating in the opposite direction during bending (Fig. 5D, Fig. 7). Therefore, the angular excursion of the tail was found to be predictive of the direction of a fast start.

DISCUSSION
Larval zebrafish vary the direction of a fast start in a manner similar to adult fish, but can execute this maneuver in three dimensions. The ability to control their escape trajectory in elevation is compatible with current thinking about the motor control of the fast start, but requires an additional means for control. Our measurements offer a basis for considering the neurobiology and biomechanics of this 3D directional control in larval fish.

The kinematics of a 3D fast start
Larval zebrafish vary the azimuth of a fast start with kinematic differences that are similar to adult fish. Adult goldfish show a positive correlation between yaw in stage 1 and the azimuth escape angle of a fast start (Eaton et al., 1991), which is similar to our results (Fig. 4B). Our findings are also consistent with the observation that a rostral stimulus creates larger head yaw and a greater change in direction than a caudal stimulus in both larval

(Liu and Fetcho, 1999) and adult fish (Foreman and Eaton, 1993). Although zebrafish larvae can exhibit a comparable change in yaw during stage 1 (Fig. 4B), the maximum azimuth angle that can be attained is smaller than in adults. Despite such differences, which are likely to stem from scale-dependent mechanics, both larvae and adults turn left or right to a greater degree by yawing more in stage 1. This common feature in kinematics justifies the use of larval fish to study the neuromechanical mechanisms of control in all fishes.

The elevation of a fast start in larvae is related to dorsoventral motion of the head and tail. During stages 1 and 2, nearly all variation in elevation can be predicted from changes in the pitch angle of the head (Fig. 4C). Therefore, as the head yaws laterally in stage 1, it simultaneously pitches towards the elevation of the maneuver's heading (Fig. 4C). This pitching motion occurs when the tail bends to momentarily form a shallow 'C' shape that is concave towards the dorsal or ventral directions. The degree of this dorsoventral bending varied with the elevation of the trajectory, as indicated by the angular excursion of the tail (Fig. 8B). In contrast to the oscillations in yaw that correlate with the azimuth of the escape, the pitching of the head proceeds in a similar direction throughout the three stages of a fast start (Figs 2, 4).

These kinematics may be summarized by the events in each stage for a particular fast start. Consider a case where a larva dives down and to the left (Fig. 9A) with direction motion that begins in stage 1. As the body curls together, the head pitches downwards and
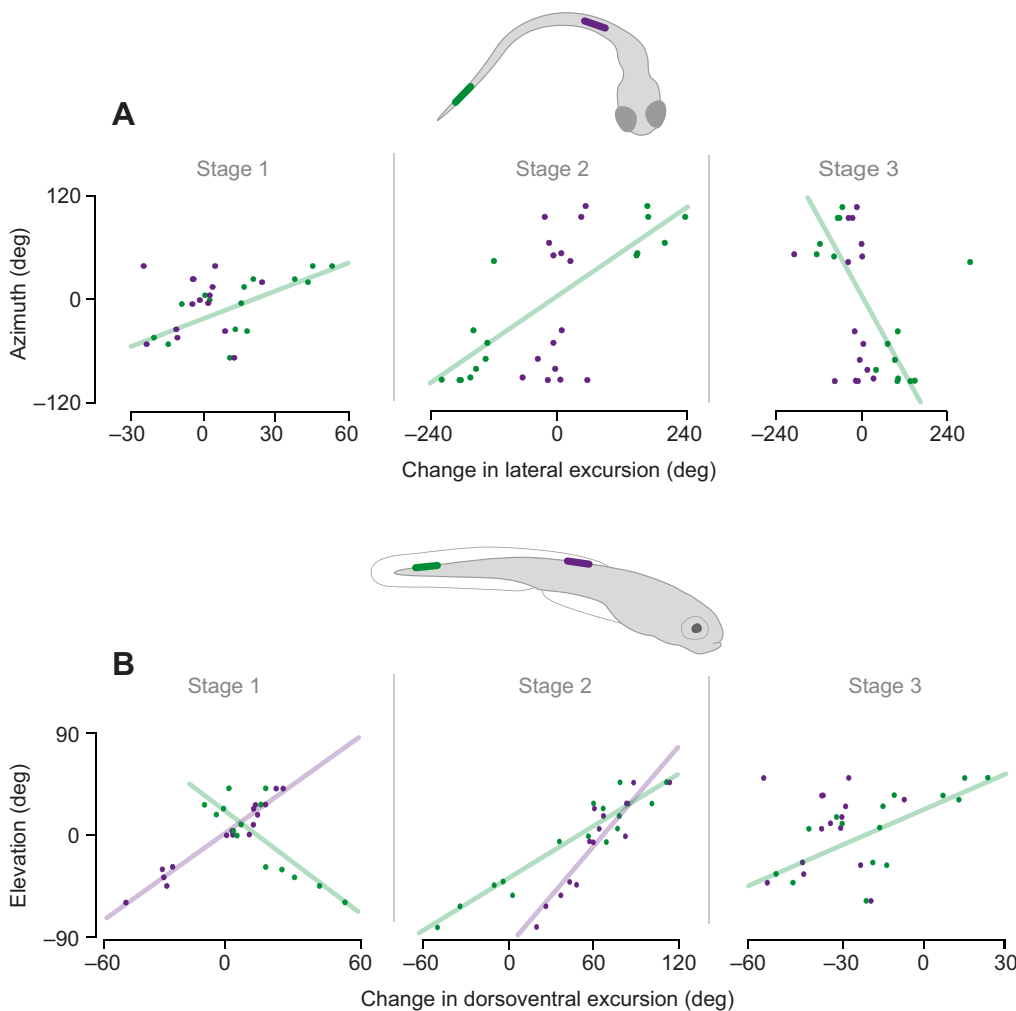
Fig. 8. The relationship between body bending and the direction of a fast start. The total angular excursion for the tail in the anterior (0.1L, in purple) and posterior (0.9L, in green) region of the tail in the lateral (A) and dorsoventral (B) directions for the stages of numerous (N=15) fast starts. (A) We found a significant correlation (P≪0.001) between the lateral excursion of the tail and the azimuth of the escape trajectory for the posterior (0.9L, in green) region of the tail during stage 1 (y=1.48x+11.5, r^2=0.90), stage 2 (y=0.428x+2.86, r^2=0.85) and stage 3 (y=0.56x−19.6, r^2=0.81). (B) Variation in the elevation of an escape could be well predicted from the dorsoventral excursion of the tail. Correlations were significant (P<0.001) for both regions of the tail and for all stages of the fast start for stage 1 (anterior: y=1.40x+0.78, r^2=0.65; posterior: y=−1.48x+11.5, r^2=0.96) and stage 2 (anterior: y=1.58x+0.34, r^2=0.85; posterior: y=0.83x+10.9, r^2=0.90). The dorsoventral excursion of the posterior of the tail only explains about half the variation in elevation (y=1.06x−22.8, r^2=0.49).

the tail bends in a concave-ventral direction. Therefore the combined pitch and yaw of the head in stage 1 sets the body in the general direction of its ultimate heading (Fig. 9A,B). During stage 2, the head reverses direction in yaw, but its pitching continues along a downward path (Fig. 9C). This will continue into stage 3 as the head continues to oscillate in yaw (Fig. 9D).

Our measurements indicate that zebrafish larvae are capable of executing a fast start with substantial 3D motion. This was reflected in the elevation of the trajectory, which spanned almost 60 deg both upwards and downwards (Fig. 4C). It was the intent of our experimental design to stimulate swimming to observe variation for the full range of potential directions. However, zebrafish larvae may vary elevation to a lesser degree under more natural conditions. For example, larvae respond to the flow generated by a predator's approach in the dark with a fast start (Stewart et al., 2014). When positioned ventral to the predator, larvae move downward at an angle of less than 30 deg and larvae positioned dorsal to the predator move with planar motion. Therefore the variation in elevation that we presently observed indicates the scope of possible 3D responses, rather than the directions that may occur in an encounter with a predator. Nonetheless, 3D escapes may be strategically beneficial for a prey (Domenici et al., 2011). A trajectory that varies in elevation will be less predictable than planar motion and downward swimming has the potential to offer refuge in the benthos. In addition, the locomotor system of a predator may be more capable of tracking prey with purely lateral motion.

Implications for motor control

The present results offer the opportunity to consider the motor control of elevation. Thinking about the directional control of the fast start has been greatly influenced by a model proposed by Foreman and Eaton, which focuses on the reticulospinal neurons that activate the motor neurons of the axial myomeres (Foreman and Eaton, 1993). Based on experimental results in adult goldfish, the Mauthner neuron and two serial homologs activate the musculature for stage 1 on the side of the body contralateral to a stimulus. With a slight delay, stage 2 muscles are activated on the ipsilateral side with unidentified command neurons. According to Foreman and Eaton, variation in direction is generated by the differential sensitivity of the command neurons to the direction of a stimulus. A rostral stimulus is predicted to activate stage 1 neurons (i.e. the Mauthner and homologs) to maximally recruit contralateral musculature and thereby create a large yaw away from the stimulus. This change in heading would consequently be maintained by a relatively modest recruitment of the stage 2 neurons and associated ipsilateral muscles. In contrast, a caudal stimulus is predicted to generate a modest recruitment in stage 1 and a relatively large recruitment in stage 2 to direct swimming forward. Therefore, the fast start may be controlled to generate swimming in a full range of azimuth angles by varying the intensity and timing of activation in these pathways. We have currently observed that zebrafish larvae also direct their swimming at a variety of azimuth angles (Fig. 4B) and previous results have shown that the azimuth can be directed away from a
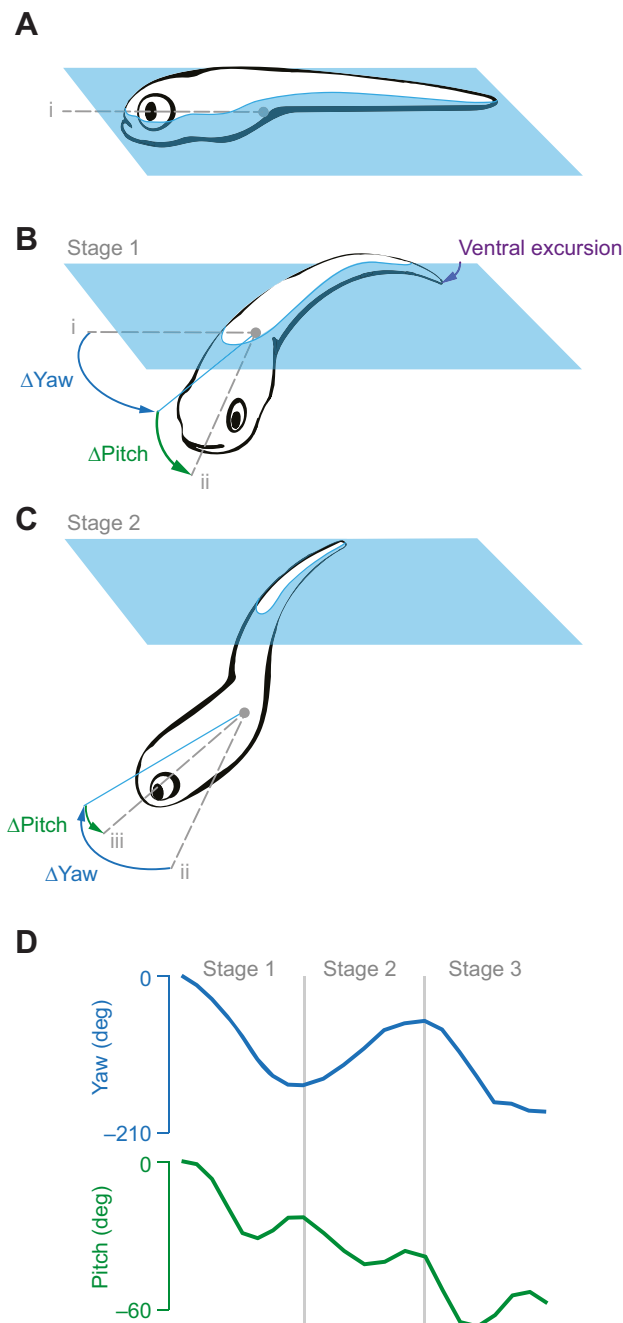
Fig. 9. Changes in elevation during a fast start. The results of our kinematic measurements support a model for the control of elevation in a fast start that is illustrated for a fast start that is directed downwards and towards the left side of the body. (A) Angular changes in the body are defined relative to its initial orientation, given by the orientation of the head (dashed gray line) and frontal plane of the body (in blue). (B) The elevation begins to adopt its course as the head changes pitch (in green) in stage 1, which continues in stages 2 (C) and 3 (not shown). Throughout these stages, the undulatory motion of the tail follows the downward course set by the head. (D) The temporal changes in yaw (blue curve) and pitch (green curve) are illustrated for the schematic motions shown above.

present results. By taking advantage of the transparent bodies of these animals, calcium imaging served to establish the patterns of activity by the Mauthner neuron and its homologs. In support of the model, all three of these neurons are activated by a rostral stimulus, but only the Mauthner neuron plays a role in response to a caudal stimulus (O'Malley et al., 1996). Experimental manipulations have shown that the fast start can be generated without the Mauthner neuron and its homologs with only subtle differences in kinematics (Kimmel et al., 1980; Liu and Fetcho, 1999). Nonetheless, it is a reasonable inference that descending commands from the hindbrain serve to activate the contralateral and ipsilateral motor neurons that drive a fast start in a manner similar to that proposed by Foreman and Eaton. It follows that muscle activation that results from these commands would need to be modulated to permit control of elevation.

Recent work on the functional organization of motor circuits in zebrafish may help to explain the neuromuscular control of elevation. The myomeres that generate tail bending are innervated by separate pairs of primary motor neurons for the epaxial (dorsal to the horizontal septum) and hypaxial (ventral to the horizontal septum) regions (Westerfield et al., 1986; Menelaou and McLean, 2012). The timing and intensity of the firing within the epaxial neurons may be varied independently from the hypaxial neurons (Bagnall and McLean, 2014). Differential activation of these motor neurons is mediated by a spinal 'microcircuit' that alters motor neuron activation during swimming, which presumably alters muscular force. These differences in activation are stimulated by input from the vestibular system when zebrafish fail to maintain equilibrium. These microcircuits do not generate descending motor commands, but rather modulate the intensity of these commands during swimming, and this modulation can be sustained over multiple tail beats.

Our results are consistent with a role for spinal microcircuits in controlling the elevation of a fast start. For example, consider the events that occur when a larval fish executes a diving maneuver (Fig. 9). The pitching motion that directs swimming downwards could be generated by the hypaxial musculature generating greater force than the epaxial musculature along the length of the tail. Such would be the result of a microcircuit command that inhibited the primary motor neurons for the epaxial muscles while exciting the hypaxial muscles. This influence on the motor commands would span the stages of a fast start and explain how the pitching of the body is maintained throughout the maneuver (Fig. 9D). An advantage to this mechanism of control is that it allows for variation in elevation without hindering the speed of the fast start.

It is possible that elevation control may be applied to more than just larval zebrafish. The experimental designs of past studies have generally neglected a consideration of elevation. The fast start of freely swimming fish, which has mostly focused on adults, is commonly studied in shallow water or with video recordings of only a dorsal perspective. Fictive preparations for neurophysiology necessarily restrict body motion and have also neglected dorsoventral motion. Therefore, it remains possible that the fast start occurs in three dimensions among other species and stages of growth. The fast start may indeed be a more complex and evasive maneuver than previously appreciated.

predator (Stewart et al., 2014). This offers further evidence that larval fish are capable of controlling the azimuth of an escape in a similar manner to adults.

Neurophysiological studies on larval zebrafish that have tested the Foreman and Eaton model inform our interpretation of the

References

Akerboom, J., Chen, T.-W., Wardill, T. J., Tian, L., Marvin, J. S., Mutlu, S., Calderon, N. C., Esposti, F., Borghuis, B. G., Sun, X. R. et al. (2012). Optimization of a GCaMP calcium indicator for neural activity imaging. *J. Neurosci.* **32**, 13819-13840.

Bagnall, M. W. and McLean, D. L. (2014). Modular organization of axial microcircuits in zebrafish. *Science* **343**, 197-200.

Barlow, G. W. (1968). Modal action patterns. In *How Animals Communicate* (ed. T. A. Seboek), pp. 261-268. Bloomington, IN: University Press.

Craig, J. J. (1989). *Introduction To Robotics: Mechanics and Control*. New York: Addison-Wesley.

Domenici, P. and Blake, R. W. (1997). The kinematics and performance of fish fast-start swimming. *J. Exp. Biol.* **200**, 1165-1178.

Domenici, P., Blagburn, J. M. and Bacon, J. P. (2011). Animal escapology I: theoretical issues and emerging trends in escape trajectories. *J. Exp. Biol.* **214**, 2463-2473.

Eaton, R. C. and Emberley, D. S. (1991). How stimulus direction determines the trajectory of the Mauthner-initiated escape response in a teleost fish. *J. Exp. Biol.* **161**, 469-487.

Eaton, R. C., Lavender, W. A. and Wieland, C. M. (1981). Identification of mauthner-initiated response patterns in goldfish: evidence from simultaneous cinematography and electrophysiology. *J. Comp. Physiol. A* **144**, 521-531.

Eaton, R. C., DiDomenico, R. and Nissanova, J. (1988). Flexible body dynamics of the goldfish c-start: implications for reticulospinal command mechanisms. *J. Neurosci.* **8**, 2758-2768.

Eaton, R. C., DiDomenico, R. and Nissanov, J. (1991). Role of the mauthner cell in sensorimotor integration by the brain stem escape network. *Brain Behav. Evol.* **37**, 272-285.

Fetcho, J. R., Higashijima, S.-I. and McLean, D. L. (2008). Zebrafish and motor control over the last decade. *Brain Res. Rev.* **57**, 86-93.

Foreman, M. B. and Eaton, R. C. (1993). The direction change concept for reticulospinal control of goldfish escape. *J. Neurosci.* **13**, 4101-4113.

Hedrick, T. L. (2008). Software techniques for two- and three-dimensional kinematic measurements of biological and biomimetic systems. *Bioinspir. Biomim.* **3**, 034001.

Kimmel, C. B., Eaton, R. C. and Powell, S. L. (1980). Decreased fast-start performance of zebrafish larvae lacking Mauthner neurons. *J. Comp. Physiol. A* **140**, 343-350.

Liu, K. S. and Fetcho, J. R. (1999). Laser ablations reveal functional relationships of segmental hindbrain neurons in zebrafish. *Neuron* **23**, 325-335.

Menelaou, E. and McLean, D. L. (2012). A gradient in endogenous rhythmicity and oscillatory drive matches recruitment order in an axial motor pool. *J. Neurosci.* **32**, 10925-10939.

Müller, U. K. and van Leeuwen, J. L. (2004). Swimming of larval zebrafish: ontogeny of body waves and implications for locomotory development. *J. Exp. Biol.* **207**, 853-868.

Nakayama, H. and Oda, Y. (2004). Common sensory inputs and differential excitability of segmentally homologous reticulospinal neurons in the hindbrain. *J. Neurosci.* **24**, 3199-3209.

Nissanov, J., Eaton, R. C. and DiDomenico, R. (1990). The motor output of the Mauthner cell, a reticulospinal command neuron. *Brain Res.* **517**, 88-98.

O'Malley, D. M., Kao, Y.-H. and Fetcho, J. R. (1996). Imaging the functional organization of zebrafish hindbrain segments during escape behaviors. *Neuron* **17**, 1145-1155.

Peterson, B. W. (1984). The reticulospinal system and its role in the control of movement. In *Brain Stem Control of Spinal Cord Function* (ed. C. D. Barnes), pp. 27-86. New York, NY: Academic.

Stewart, W. J. and McHenry, M. J. (2010). Sensing the strike of a predator fish depends on the specific gravity of a prey fish. *J. Exp. Biol.* **213**, 3769-3777.

Stewart, W. J., Nair, A., Jiang, H. and McHenry, M. J. (2014). Prey fish escape by sensing the bow wave of a predator. *J. Exp. Biol.* **217**, 4328-4336.

Walker, J. A., Ghalambor, C. K., Griset, O. L., McKenney, D. and Reznick, D. N. (2005). Do faster starts increase the probability of evading predators? *Funct. Ecol.* **19**, 808-815.

Weihs, D. (1973). The mechanism of rapid starting of slender fish. *Biorheology* **10**, 343-350.

Westerfield, M. (1993). *The Zebrafish Book: A Guide for the Laboratory Use of Zebrafish (Brachydanio rerio)*. Eugene, OR: University of Oregon Press.

Westerfield, M., McMurray, J. V. and Eisen, J. S. (1986). Identified motoneurons and their innervation of axial muscles in the zebrafish. *J. Neurosci.* **6**, 2267-2277.